Dark matter annihilation from intermediate-mass black holes: Contribution to the extragalactic gamma-ray background

Shunsaku Horiuchi[*]

Department of Physics, School of Science, The University of Tokyo, Tokyo 113-0033, Japan

Shin'ichiro Ando[†]

Theoretical Astrophysics, California Institute of Technology, Pasadena, California 91125, USA,
Kellogg Radiation Laboratory, California Institute of Technology, Pasadena, California 91125, USA,
and Department of Physics, School of Science, The University of Tokyo, Tokyo 113-0033, Japan

We investigate contributions to the extragalactic gamma-ray background (EGB) due to neutralino dark matter (DM) pair-annihilation into photons, from DM density enhancements (minispikes) surrounding intermediate-mass black holes (IMBHs). We focus on two IMBH formation scenarios; our conservative scenario where IMBHs are remnants of Population-III stars, and our optimistic scenario where IMBHs are formed in protogalactic disks. In both scenarios, their formation in pregalactic halos at high redshift lead to the formation of minispikes that are bright sources of gamma-ray photons. Taking into account minispike depletion processes, we only sum contributions from a cosmological distribution of IMBHs with maintained minispikes. Our conservative scenario (BH mass $10^2 M_\odot$ with a $r^{-3/2}$ minispike) predicts gamma-ray fluxes that are an order larger than the equivalent flux, using the same DM parameters (mass 100 GeV and annihilation cross section 3×10^{-26} cm^3 s^{-1}), from the host halo without IMBH minispikes. Our optimistic scenario (BH mass $10^5 M_\odot$ with a $r^{-7/3}$ minispike) predicts fluxes that are three orders larger, that can reach current EGB observations taken by EGRET (DM parameters as above). This fact may serve interesting consequences for constraining DM parameters and elucidating the true nature of IMBHs. Additionally, we determine the spectra of DM annihilation into monochromatic gamma rays, and show that its flux can be within observational range of GLAST, providing a potential "smoking-gun" signature of DM.

I. INTRODUCTION

Despite compelling indirect evidence, from galactic to cosmological scales, the fundamental nature of the dominant nonbaryonic component in the matter density of the Universe (dark matter, hereafter DM) remains unknown. Intriguingly, extended models of particle physics independently provide us with a host of particle candidates for this as yet unknown matter, of which the most popular is the supersymmetric neutralino (see reviews [1–3] for details). Upgrades of underground direct detectors looking for scattering of DM particles from nuclei, together with future neutrino, antimatter, and gamma-ray detectors looking for products of DM annihilation, will dramatically enhance our chances of understanding the true nature of DM. In particular, the forthcoming launch of the Gamma Ray Large Area Space Telescope (GLAST) [4] and numerous ground based Atmospheric Cerenkov Telescopes make indirect gamma-ray search especially promising.

Since the DM annihilation rate scales as the DM density squared, there is great advantage in observing areas where the DM density is believed to be high. The galactic center (GC) is the immediate choice, and indeed strong gamma-ray emission has been observed and its nature and origin

have been investigated by many researchers [5–13]. However, the DM density in the GC is highly uncertain, making accurate predictions difficult. For example, DM enhancements called "spikes" can form during the formation of a central supermassive-BH (SMBH) [14], but it can also be depleted by various processes by varying degrees [15–18]. In addition, nearby astrophysical (non-DM) gamma-ray sources make a potential DM detection impossible for all but a narrow range of DM parameters [19]. Intermediate-mass black holes (IMBHs, see e.g. [20]) provide an alternative source that may work positively for DM detection. Bertone *et al.* [21] recently investigated the possibility of detecting a "smoking-gun" gamma-ray signature of DM using IMBHs in the Milky Way as point sources. They showed that IMBH formation increases the DM density in its vicinity to produce a "minispike," and also that DM enhancement depletion processes are generally less significant for IMBHs due to their roughly spherical distribution about the GC. They conclude that under optimistic circumstances, the Energetic Gamma Ray Experimental Telescope (EGRET) may have already seen a few of the IMBH minispikes as unidentified sources.

Another avenue of indirect DM search is via the extragalactic gamma-ray background (hereafter EGB) measured over a wide energy range [22,23]. The origin of this background is currently unknown, and it has been speculated that DM annihilation gamma rays from cosmo-

---
[*]Electronic address: horiuchi@utap.phys.s.u-tokyo.ac.jp
[†]Electronic address: ando@tapir.caltech.edu

logical distributions of DM contribute to some degree [24–31]. Since the DM annihilation cross section is so small, a consideration of DM enhancements is crucial for meaningful gamma-ray flux predictions. A popular DM enhancement is those at the centers of galactic DM halos. However, Ando [29] has recently shown that they are strongly constrained by observations of our galaxy. The author assumes universality of galactic DM halo profiles, and shows that DM annihilation cannot significantly contribute to the EGB without exceeding gamma-ray observations from our GC [29]. The author also points out that this constraint could be loosened when one takes DM substructures into account.

In this paper we argue IMBHs minispikes as a *substructure in the DM halo, that can lead to enhancements that do not conflict with current observations of our galaxy.* We determine contributions to the EGB from IMBH minispikes by summing gamma-ray fluxes from all redshifts. IMBH minispikes are not expected to greatly suffer from depletion processes, but we do take into account BH-BH mergers, which are known to strongly deplete minispikes and do occur in IMBHs. We also consider a conservative case ($10^2 M_\odot$ BHs of Population-III origin [32] with a $r^{-3/2}$ minispike) and an optimistic case ($\sim 10^5 M_\odot$ BHs formed in the centers of protogalactic disks [33] with a $r^{-7/3}$ minispike). Our result is that contributions to the EGB are increased by 1–3 orders in magnitude. In particular, our optimistic case predicts fluxes that can reach current EGB observations. As this has interesting implications for constraining DM parameters and IMBH scenarios, we critically assess uncertainties in our calculation. We then determine the flux of DM annihilation into line gamma rays, and show that under optimistic conditions, it is observable by GLAST. This provides a potential smoking-gun signature of DM.

This paper is structured as follows. In Sec. II we introduce IMBHs, starting with their existence, followed by their formation scenarios, and finishing off with a summary of recent numerical studies. Then in Sec. III we develop our calculation frameworks, first for the EGB, followed by DM annihilation, then minispike formation, moving finally on to our IMBH number density fitting. Calculations and results are in Sec. IV, and discussions and conclusions in Sec. V. In all our calculations we adopt the standard flat cosmological constant plus cold DM (ΛCDM) cosmology, with $\Omega_M = 0.3$, $\Omega_\Lambda = 0.7$, $h = 0.7$, and $\sigma_8 = 0.9$.

II. IMBH: EVIDENCE AND PROPERTIES

A. Evidence for IMBH

Clues for the existence of a class of BHs with masses heavier than stellar BHs but lighter than supermassive black holes (SMBH) have accumulated in recent years. We call these BHs intermediate-mass BHs (IMBHs) and loosely define their mass range as $20 \lesssim M_{bh}/M_\odot \lesssim 10^6$.

We briefly discuss the observational evidences and theoretical motivations for their existence.

Observationally, studies of objects known as ultraluminous x-ray sources (ULXs, [34,35]) reveal that they may harbor IMBHs. Although most x-ray sources can be understood as accretion by compact objects such as BHs, there is an upper limit on the luminosity for a given BH mass, known as the Eddington limit. For $20 M_\odot$, commonly accepted as the upper limit of stellar BHs, this limit is $\sim 2.8 \times 10^{39}$ ergs s^{-1}. ULXs are observed to exceed this limit. This phenomena can be explained by several mechanisms, including a short-term super-Eddington phase [36], beaming [37], or normal accretion by an IMBH. Although the debate has not been settled, evidence favoring the IMBH mechanism over the other two has accumulated in recent years; these come in various forms, including spectral analysis [20,38], evidence for a low temperature (~ 0.1 keV) black-body component [39], analysis of break frequencies of the power density spectrum [40], and observation of broad Fe lines and quasiperiodic oscillations (QPO) [41]. It seems that at least a fraction of the ULXs, in particular, the most luminous ones, are IMBHs. The BH mass inferred from ULX observations is of the order $\sim 10^3 M_\odot$ (assuming no beaming and accretion efficiency $\sim 10\%$). Also, from their positions in the host galaxies we can deduce an upper limit of $\lesssim 10^6 M_\odot$, in order not to sink to the galactic center by dynamical friction within a Hubble time [20].

Theoretically, the existence of a population of IMBHs helps explain the origin of SMBHs. There is as yet no definitive SMBH formation scenario, but the discovery of quasars at redshifts $z \approx 6$ in the Sloan Digital Sky Survey [42–46] suggests that they were already formed at high redshifts. Such an early formation lends itself to scenarios with massive seed-BHs, frequent mergers, and rapid accretion. A hierarchical formation scenario starting from massive seed-BHs also helps explain the tight correlations observed between the SMBH mass and properties of the host galaxy and halo [33]. The natural outcome of this hierarchical scenario is the existence of "wandering" BHs in galactic halos, resulting from seed-BHs that did not successfully merge into a SMBH [47–49], which we call IMBHs. However, despite the theoretical interests, it is difficult to obtain conclusive evidence for their existence. One viable strategy is to search for gravitational waves produced in seed-BH mergers, which may become possible with the launch of the Laser Interferometer Space Antenna (LISA) [48,50].

B. IMBH formation scenarios

In this study, we follow a previous study by Bertone *et al.* [21] and focus on two seed-BH formation scenarios covering the wide range of possible IMBH masses. In the first scenario, which we refer to as scenario A, the seed-BHs are remnants of the collapse of Population-III (or first

generation) stars [32]. These stars are generally massive due to suppression of mass-loss processes, a result of their very low-metal composition. As such, they are also called zero-metalicity or very massive stars (VMS). The fate of VMS have been studied by e.g. [51,52]: stars with $100 \lesssim M/M_\odot \lesssim 250$ encounter the electron-positron pair instability and explode in a giant nuclear-powered explosion, leaving no compact remnant, while heavier stars collapse completely to a BH containing at least half of the stellar mass [52].

What we need to know is the mass-function of these BHs. Unfortunately, the mass-function of Population-III stars is not well known, although recent studies indicate a double peaked function that extends up to a few $10^3 M_\odot$ [53]. We base our scenario on the one proposed in [32] and further studied by [21,47,49,54]. Interestingly, if BHs with masses $\gtrsim 10^2 M_\odot$ form at high redshifts in minihalos representing $\sim 3\sigma$ peaks of the smoothed density field, the resulting baryon mass fraction is found to be comparable to those observed for SMBHs in nearby galaxies [32]. As in [21], we conservatively consider BHs of mass $10^2 M_\odot$ forming in minihalos of masses larger than $M_{\nu,\text{crit}} \sim 10^7 M_\odot$ at formation redshift $z_f \sim 18$.

In the second scenario, which we refer to as scenario B, BHs form from low angular momentum gas in protogalactic disks at high redshifts, producing a population of seed-BHs with masses $\sim 10^5 M_\odot$. We use the scenario proposed in [33], which we briefly summarize. During the collapse of the first halos, gas cools and a pressure supported disk forms if the halo is massive enough to contain a relatively large fraction of molecular hydrogen (molecular hydrogen is the main coolant, see [55]). Local gravitational instabilities in the disk manifest themselves as an effective viscosity that transfers angular momentum outwards and cause an inflow of gas, in particular, the low angular momentum tail. In halos that are both massive enough to contain enough hydrogen for cooling *and* do not experience mergers with other halos, the protogalactic disk can evolve uninterrupted until ultimately being terminated by the heating and disruption caused by supernovae of Population-III stars. During this time, mass transfer of order $\sim 10^5 M_\odot$ occurs. The central mass may be briefly pressure supported but will ultimately collapse to a BH due to post-Newtonian instabilities. Since Population-III stars have typical lifetimes of 1–10 Myrs, the halo must be avoid of mergers over many dynamical times. This sets a stringent lower limit on the required halo mass. At $z_f = 12$, this limit is $M_{\nu,\text{crit}} = 10^8 M_\odot$ (see [33] for an expression). The masses of the BHs that form have a near log-normal distribution with peak mass $M_{\text{bh},0} = 2.3 \times 10^5 M_\odot$ independent of z_f, with spread $\sigma_{\text{bh}} = 0.9$ [33].

Scenario B naturally contains many parameters other than z_f (such as fraction of gas cooled, lifetime of Population-III stars, etc.). However, uncertainties in these parameters largely affect $M_{\text{bh},0}$, and as such are ultimately masked by uncertainties in z_f, which affects the *total number* of seed-BHs formed. We therefore treat scenario B formation to be described by one parameter, z_f. Now, the epoch of cosmological reionization places a lower limit on z_f. This is because the heating of the intergalactic medium and the subsequent ionization of molecular hydrogen (i.e. reionization) terminates further baryon cooling. Without molecular hydrogen, scenario B formation cannot proceed, even in the heaviest halos which satisfy $M_\nu > M_{\nu,\text{crit}}$. Therefore, for scenario B, $z_f = z_{\text{re}}$, where z_{re} is the redshift of reionization (we assume for simplicity that seed-BH formation stops abruptly at reionization).

C. IMBH number density: Results from numerical studies

Now that we have discussed IMBH formation, we will summarize how their number density evolves with time. Since in this work we are only interested in IMBHs with minispikes, from here on we will use "IMBH" to imply "an IMBH with a maintained minispike." First, although seed-BH formation can lead to minispike formation, various processes destroy it by varying degrees (see Sec. III C), and the strength and number of minispikes decrease with time. BH mergers, i.e. mergering with another IMBH or a SMBH, are the most destructive and we must therefore consider its effects. Before doing so however (in Sec. III D) we summarize basic procedures and results of previous numerical studies.

The basic approach focuses on constructing a statistical sample of halo formation histories (each called a "realization") in the context of the hierarchical CDM model for structure formation, followed by computing the dynamical evolution of halos and BHs within halos (see [21,47,48,56] for further details). The first step is to consider a virialized halo of mass $M_{\nu,0}$ at $z = 0$ and construct a merger history, i.e. a list of all the smaller halos that merged together to form the final halo, as well as the redshifts at which the mergers occurred. The next step is to plant BHs in halos that satisfy seed-BH formation conditions. That is, if a halo satisfies $M_\nu > M_{\nu,\text{crit}}$ and $z > z_f$, a seed-BH is planted at the earliest time $M_\nu > M_{\nu,\text{crit}}$ still holds. This point is labeled z_{bh}. The last step involves evolving the halos and BHs forward to $z = 0$, as described in [48,56]. During the last step, a BH that comes within a distance $\min(0.01 r_{\text{vir}}, 1 \text{ kpc})$, where r_{vir} is the virial radius of the halo, of another BH is considered a BH-BH "potential pair," and is decoupled from the simulation. Previous work focused on the gravitational waves produced by the potential pairs' subsequent mergers [48], but for our purposes we exclude all potential pairs from our EGB calculation.

What necessary results can we obtain from these studies? First, the distribution of BH formation redshifts z_{bh} is found to be exponential, i.e. using the Milky Way galaxy

with $M_{\nu,0} = 10^{12.1}h^{-1}M_\odot$ and 200 realizations, [48] finds that the number of BHs formed peaks at z_f and decreases exponentially for higher z_{bh} (see their Fig. 2). Second, by following the dynamical evolution of BHs, [21] finds that $N_{bh,A} = 1027 \pm 84$ scenario A BHs and $N_{bh,B} = 101 \pm 22$ scenario B BHs remain unmerged in a Milky Way-sized halo. Errors denote the 1σ halo-to-halo scatter (200 realizations were performed). Finally, [48] finds that the number of potential pairs formed is highest at z_f when the BH number density is largest, and decreases as a power-law of $(1 + z)$ with decreasing z (see their Fig. 3).

III. FORMULATIONS

A. Extragalactic gamma-ray background

To calculate contributions to the EGB flux from unresolved cosmological DM sources, we adopt the methodology in Ullio *et al.* [25], but extend it for our purposes of including IMBH minispike enhancements.

Let $d\mathcal{N}_\gamma/dE(E, M_{bh}, z)$ be the differential energy spectrum for the number of gamma-ray photons emitted per unit time from a single IMBH of mass M_{bh} at redshift z, and $dn/dM_{bh}(M_{bh}, z)$ the comoving number density of IMBHs of mass M_{bh} at redshift z. From these we can determine the number of photons emitted in a proper volume dV say, at redshift z in time interval dt and energy range $(E, E + dE)$. Then, assuming isotropic emission, the corresponding number of photons dN_γ collected by a detector on Earth with an effective area dA in the redshifted energy range $(E_0, E_0 + dE_0)$ over a time dt_0, is

$$dN_\gamma = \int dM_{bh}(1 + z)^3 \frac{dn}{dM_{bh}}(M_{bh}, z)\frac{d\mathcal{N}_\gamma}{dE}$$
$$\times (E, M_{bh}, z)e^{-\tau(E_0,z)}\frac{dVdA}{4\pi(R_0 r)^2}dE_0 dt_0, \quad (1)$$

where we have used the fact that $dEdt = (1 + z)dE_0(1 + z)^{-1}dt_0 = dE_0 dt_0$. The exponential term is an attenuation factor which accounts for the absorption of gamma rays during propagation to Earth, the factor $(1 + z)^3$ converts from comoving to proper IMBH number density, and R_0 comes from the metric of our cosmology as defined in Sec. I. We define dV by radial increment dr and angular increment $d\Omega$ as

$$dV = \frac{(R_0 r)^2 R_0}{(1 + z)^3}drd\Omega.$$

The main absorption of gamma rays of a few GeV is via pair production on the extragalactic background light emitted by galaxies in the optical and infrared bands. Although at these gamma-ray energies attenuation is almost negligible, we use the form $e^{-z/z_{max}}$, where we approximate $z_{max} \simeq 3.3(E_0/10 \text{ GeV})^{-0.8}$, which is a parametrization that reproduces results of [57] with enough accuracy. Substituting dV into Eq. (1) and changing the integration along the line of sight dr to along dz, we get for the flux

$$\frac{d\Phi_\gamma}{dE_0} \equiv \frac{dN_\gamma}{dAd\Omega dt_0 dE_0}$$
$$= \frac{c}{4\pi}\int dz \frac{e^{-z/z_{max}}}{H_0 h(z)}\int dM_{bh}\frac{dn}{dM_{bh}}(M_{bh}, z)\frac{d\mathcal{N}_\gamma}{dE}$$
$$\times (E_0(1 + z), M_{bh}, z), \quad (2)$$

where c is the speed of light, H_0 is the Hubble parameter now, and $h(z)$ is the function $h(z) = \sqrt{[\Omega_M(1 + z)^3 + \Omega_\Lambda]}$.

We use Eq. (2) to compute the final EGB flux. In the following subsections, we will deal with the physical quantities in the expression in detail.

B. Dark matter annihilation gamma rays

In order for DM particles to satisfy cosmological constraints, they are expected to have a small but nonzero annihilation cross section into standard model particles. This ensures they are in chemical equilibrium in the early universe. By constraining their relic density by cosmological observations, one can obtain limits on their annihilation cross section. For DM that is a thermal relic, the required cross section is 3×10^{-26} cm^3 s^{-1}. However this should be taken as an upper limit, because processes such as coannihilation can allow smaller cross sections (see [1,3] for details). The DM particle mass is constrained from below by collider experiments and above by theory, giving a commonly accepted range of $m_\chi \sim 50$ GeV–10 TeV.

Now, the flux of gamma rays from a single IMBH minispike is quantified by the term $d\mathcal{N}_\gamma/dE(E, M_{bh}, z)$ in Eq. (2). For gamma rays of DM origin, we can rewrite

$$\frac{d\mathcal{N}_\gamma}{dE} = \frac{\sigma v}{2}\frac{dN_\gamma(E)}{dE}\int_{r_{lim}}^{r_{sp}} n_\chi^2 d^3 r$$
$$= \frac{\sigma v}{2}\frac{dN_\gamma(E)}{dE}\frac{1}{m_\chi^2}\int_{r_{lim}}^{r_{sp}} \rho^2(r)d^3 r, \quad (3)$$

where the factor $1/2$ appears due to the fact this is an annihilation of identical particles [25], $\rho(r)$ is the DM density profile around an IMBH ranging from radii r_{lim} to r_{sp} (we discuss these in Sec. III C), σv is the annihilation cross section times relative velocity, and $dN_\gamma(E)/dE$ is the differential gamma-ray yield per annihilation. The latter can be divided into continuum and monochromatic (line) emissions, and can be written as [25]

$$\frac{dN_\gamma(E)}{dE} = \sum_Y b_{\gamma Y}n_{\gamma Y}\delta(E - m_\chi(1 - M_Y^2/4m_\chi^2))$$
$$+ \sum_F b_F \frac{dN_{cont}^F}{dE}(E), \quad (4)$$

where the second term refers to the continuum. The continuum photons are produced by annihilation into the full set of tree-level final states F including fermions and gauge or Higgs bosons which generate photons on decay. The

bulk of the photons however are produced in the hadronization and decay of neutral pions (decay mode $\pi^0 \to 2\gamma$), with a branching ratio of $b_F = 98.8\%$. The monochromatic emission on the other hand is the result of prompt annihilation into two-body states including a photon, a process that is forbidden at tree-level and only allowed in higher order perturbation theory. Although subdominant, these gamma rays have the advantage of producing a smoking-gun signature of DM annihilation, i.e. photons of energy $E = m_\chi$ for the 2γ final state and $E = m_\chi(1 - M_Y^2/4m_\chi^2)$ for the photon and particle Y final state. The parameter $b_{\gamma Y}$ is the branching ratio into the respective channels, and $n_{\gamma Y}$ is the number of photons emitted per annihilation.

In the current work we consider both the continuum and monochromatic gamma-ray emissions. For the continuum we consider the π^0 branch, and use a conveniently parametrized form of the rest frame energy distribution per annihilation, $dN_{cont}(E)/dE = (0.42/m_\chi)e^{-8x}/(x^{1.5} + 0.000\,14)$ where $x \equiv E/m_\chi$. For the monochromatic emission we consider the $\chi\bar{\chi} \to 2\gamma$ process, which exists in many supersymmetric models. We use for the branching ratio $b_{2\gamma} = 10^{-3}$.

C. Dark matter enhancement around IMBH

The emergence of a deeper gravitational potential due to the formation of a BH inevitably alters the DM halo in which it is formed. It has been shown that the adiabatic formation of a SMBH results in an enhancement of the nearby DM density, called a "spike" [14]. However, it has also been shown that spike formation depends on initial conditions [15], and even formed, it is depleted by processes such as BH-BH mergers [16], dynamical processes such as gravitational scattering off stars [18], and DM annihilation itself [17]. Fortunately, minispikes around IMBHs may not be greatly affected by these problems. First, we have selected IMBHs that survive without experiencing any major mergers. Second, these unmerged IMBHs are not necessarily localized in the galactic center, and null observations of ULXs in our galaxy suggest they reside in satellite halos with no significant stellar component. These imply that dynamical processes are not very significant. Third, a central BH formation is a built-in property of scenario B, predicting a strong minispike. However, we must make clear that the precise likelihood of minispike formation and survival are still uncertain. With these in mind, we treat scenario B as our optimistic case and scenario A our conservative.

The BH in scenario B forms in the center of its host halo [33], and therefore predicts a strong minispike. To compute its shape we need to specify the initial DM profile. If we write the initial inner DM profile as $\rho(r) \propto r^{-\gamma}$, the minispike has the form [21]

$$\rho_{sp}(r) = \rho(r_{sp})\left(\frac{r}{r_{sp}}\right)^{-\gamma_{sp}}, \qquad (5)$$

where r_{sp} is the radius of the minispike and γ_{sp} is the gradient, given as

$$\gamma_{sp} = \frac{9 - 2\gamma}{4 - \gamma}. \qquad (6)$$

Values for γ have been proposed by analytic fits of N-body simulations, e.g. $\gamma = 1$ by Navarro, Frenk, and White (NFW) [58], and $\gamma = 1.5$ by Moore *et al.* [59]. Recent simulations have produced shallower profiles (see [60] and references therein) and as well as somewhere between 1–1.5 [61–63]. In this work we assume a middle value of $\gamma = 1$, but keep in mind that a smaller value will lead to less gamma rays. For reference, our values for halo radii are summarized in Table I.

For scenario A, while some works show that they are formed in the centers of their host halos [65], others show fragmentation may lead to off-center BHs [66]. Although motivations for a central BH are strong, to remain conservative we consider an off-center BH formation. It has been shown that BH formation in a uniform DM background will form a mild $r^{-3/2}$ minispike [21,54,67,68]. Specifically, we consider the minispike studied in [21,54], with $\rho(r) = \rho_h(r/r_h)^{-3/2}$ where $r_h = 0.045$ pc.

In both scenario A and B minispikes, the very DM annihilation we are studying sets a limit on the inner minispike radius. Assuming DM annihilation is the main process by which the inner density decreases, the DM number density n_χ obeys the evolution equation $\dot{n}_\chi(r, t) = -\sigma v n_\chi^2(r, t)$. Solving this yields the solution

$$n_\chi(r, t) = \frac{n_\chi(r, t_f)}{1 + n_\chi(r, t_f)\sigma v(t - t_f)}, \qquad (7)$$

where $t - t_f$ is the time elapsed since BH formation. The upper limit is of order $m_\chi/\sigma v(t - t_f)$, and we define r_{lim} as the radius at which the following holds

$$\rho_{sp}(r_{lim}) = \frac{m_\chi}{\sigma v(t - t_f)} \equiv \rho_{lim}, \qquad (8)$$

where m_χ is the DM mass. For common DM parameters, r_{lim} has grown to $\simeq 10^{-3}$ pc by $z = 0$.

TABLE I. Representative values of halo radii for scenario B, for two formation redshifts. Shown are the halo virial radius r_{vir}, the scale radius r_s which defines the shape of the NFW profile (see [58]), the "influence" radius r_h of the BH as defined in [64], and the inner radius of the minispike r_{lim}. DM parameters are $m_\chi = 100$ GeV and $\sigma v = 3 \times 10^{-26}$ cm^3 s^{-1}.

	Radii, $z_f = 10.9$ [pc]	Radii, $z_f = 12$ [pc]
r_{vir}	1300	1100
r_s	510	480
r_h	34	33
r_{sp}	6.8	6.7
$r_{lim}(z = 0)$	5×10^{-3}	4×10^{-3}

D. Modelling the IMBH number density

Now we parametrize the decreasing IMBH number density, using results of previous numerical studies. To determine the initial (i.e. at z_f) IMBH number density, we consider a delta-function seed-BH formation occurring at z_f, and plant BHs in halos that satisfy $M_v \gtrsim M_{v,\mathrm{crit}}$. This simplified picture neglects BHs that would have formed earlier. That is, for some halos we plant one BH where in fact there would be two (or more). However, as [48] shows, the number of BHs formed in $z > z_f$ decreases exponentially. This, coupled to the fact that massive halos become increasingly unlikely for higher redshifts, the effect of ignoring them is minimal. We also stress that this picture in no way overestimates EGB contributions, because (i) we have underestimated the initial BH density, and (ii) we have neglected all DM annihilations before z_f. Moreover, any underestimation is masked by uncertainties caused by z_f.

The required calculation is

$$n_{\mathrm{bh}}(z_f) = \int_{M_{v,\mathrm{crit}}}^{\infty} dM_v \frac{dn}{dM_v}(z = z_f), \qquad (9)$$

where n_{bh} is the comoving number density of IMBHs that have not experienced any mergers, and dn/dM_v is the halo mass-function. For the mass-function we use one postulated by Press-Schechter theory [69],

$$\frac{dn}{dM} = \frac{\bar{\rho}_0}{M^2} \nu f(\nu) \frac{d\log\nu}{d\log M}, \qquad (10)$$

where $\bar{\rho}_0$ is the comoving matter background density, $\bar{\rho}_0 = \rho_c \Omega_M$, with ρ_c the critical density. The parameter $\nu \equiv \delta_{\mathrm{sc}}(z)/\sigma(M)$ is defined as the ratio between the critical linear fractional overdensity required for virialization over $\sigma(M)$ the present rms linear density fluctuation in spheres containing a mean mass M. For the multiplicity function $f(\nu)$ we use the ellipsoidal collapse model [70], normalized to results of N-body simulations of the Virgo Consortium [71], as was done in [25].

Now, we assume that the number of IMBHs present and the number of potential pairs formed are proportional, and fit a power-law redshift dependency to n_{bh},

$$n_{\mathrm{bh}}(z) = n_{\mathrm{bh}}(z_f)\left(\frac{1+z}{1+z_f}\right)^{\beta}, \qquad (11)$$

where β is a free parameter. We can derive representative values for β by fitting $n_{\mathrm{bh}}(0)$ to numerical results by [21]. From their value of $N_{\mathrm{bh},A}$ ($N_{\mathrm{bh},B}$), we interpolate the number of unmerged IMBHs in other galaxies by their halo masses, and determine $n_{\mathrm{bh}}(0)$ as

$$n_{\mathrm{bh}}(0) = N_{\mathrm{bh}} \int_{M_{v,\mathrm{crit}}}^{\infty} dM_v \left(\frac{M_v}{10^{12.1}h^{-1}M_\odot}\right)^{\alpha} \frac{dn}{dM_v}(0), \quad (12)$$

where α is some constant which we assume to be 1. This gives $\beta \simeq 0.2$ (0.3) for scenarios A (scenario B). Although in reality we do not expect α to be exactly 1 (e.g. we expect

TABLE II. Scenario A and B parameters, including formation redshift z_f, the minimum halo mass required for formation to occur $M_{v,\mathrm{crit}}$, the number density of IMBH n_{bh} at $z = z_f$ determined from Eq. (9), the number of IMBHs residing in a Milky Way-size galactic halo N_{bh} [21], n_{bh} at $z = 0$ derived from Eq. (12), and β derived from our fitting.

	Scenario A	Scenario B
z_f	18	$10.9^{+2.3}_{-2.7}$ [a]
M_{bh} [$M_\odot$]	10^2	10^5
$M_{v,\mathrm{crit}}(z_f)$ [$M_\odot$]	4×10^6	10^8
$n_{\mathrm{bh}}(z_f)$ [Mpc^{-3}]	23	2.5
N_{bh}	1027 ± 84	101 ± 22
$n_{\mathrm{bh}}(0)$ [Mpc^{-3}]	12	1.1
β	0.2	0.3

[a]z_{re} taken from Wilkinson Microwave Anisotropy Probe (WMAP) 3rd year results [72].

less unmerged IMBHs in older elliptical galaxies), we find that for reasonable deviations from $\alpha = 1$ our estimates of β do not appreciably change. Moreover, uncertainties caused by deviations in α are far smaller than those caused by z_f.

Lastly, we conclude this section with the parameters of scenarios A and B in Table II.

IV. CALCULATION AND RESULTS

A. Contribution to the EGB

Substituting Eq. (3) into Eq. (2) we find the gamma-ray flux observed at Earth as

$$\frac{d\Phi_\gamma}{dE_0} = \frac{\sigma v}{8\pi} \frac{c}{H_0} \frac{\bar{\rho}_0^2}{m_\chi^2} \int_0^{z_f} dz \frac{\Delta^2(z)}{h(z)} \frac{dN_\gamma(E')}{dE} e^{-z/z_{\max}}, \quad (13)$$

where $E' = E_0(1 + z)$ and $\Delta^2(z)$ is defined

$$\Delta^2(z) = \frac{1}{\bar{\rho}_0^2} \int dM_{\mathrm{bh}} \frac{dn}{dM_{\mathrm{bh}}}(M_{\mathrm{bh}}, z) \int_{r_{\lim}}^{r_{\mathrm{sp}}} \rho^2(r) d^3r. \quad (14)$$

Note the disappearance of the $(1 + z)^3$ term in Eq. (13) compared to [25]. The reason for this is that while the DM density in the halo is a function of z, the density in the minispike around an IMBH is only a function of z_f; the z dependence is taken into account instead by $r_{\lim}$.

For scenario B, since the BH mass distribution is near log-normal, and the enhancement due to the minispike scales linearly with the BH mass, we find that with very good accuracy we can approximate all the BH mass to have the peak value $M_{\mathrm{bh},0}$. Hence, we substitute $dn/dM_{\mathrm{bh}}(M_{\mathrm{bh}}, z) = n_{\mathrm{bh}}(z)\delta(M_{\mathrm{bh}} - M_{\mathrm{bh},0})$, which gives the final form we will use,

$$\Delta^2(z) = \frac{1}{\bar{\rho}_0^2} n_{\mathrm{bh}}(z) \int_{r_{\lim}}^{r_{\mathrm{sp}}} \rho(r)^2 d^3r. \quad (15)$$
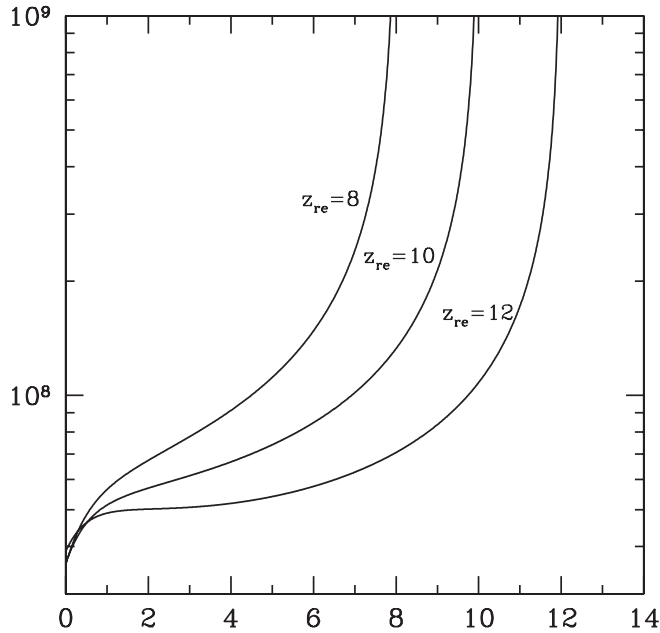
FIG. 1. Enhancement factor Δ^2 as a function of redshift, for scenario B IMBH minispikes. Three values of $z_f = z_{re}$ are plotted, 8, 10, and 12. The peak enhancement at z_f is largely due to the fact that the minispike is sharpest just after it is formed. This demonstrates the effectiveness of the minispike in enhancing contributions to the EGB.
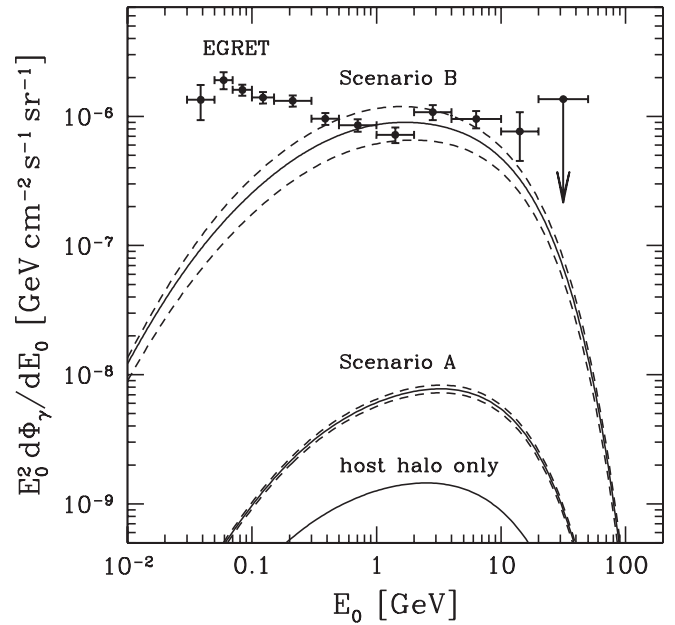

FIG. 2. Contributions to the EGB flux, from scenario A and scenario B IMBH minispikes. Also shown are EGRET data and predictions of our minimal host halo only scenario (i.e. no spikes and minispikes). We see that minispikes increase EGB contributions by 1–3 orders in magnitude. The 1σ scatter in $N_{bh,A}$ [21] is shown for scenario A. For scenario B, the 1σ scatter in $N_{bh,B}$ as well as z_{re} are shown combined. In all calculations, z_f and β shown in Table II are used, with DM parameters $m_\chi = 100$ GeV and $\sigma\upsilon = 3 \times 10^{-26}$ cm^3 s^{-1}. Note that scenario A is our conservative case; a BH of mass $10^2 M_\odot$ with a mild $r^{-3/2}$ minispike.

In Fig. 1 we show the redshift dependence of the enhancement function $\Delta(z)^2/h(z)$ for scenario B, for three values of $z_f = z_{re} = 8$, 10, and 12. The strongest enhancement occurs at z_f, partly because of the highest IMBH number density, but mainly because of the presence of the sharpest minispike. This displays the merits of considering the EGB, because high redshift enhancements are most easily observed as a diffuse background. On the other hand, we must therefore carefully consider the IMBH number density at z_f. However, a major uncertainty in the hierarchical formation scenario of SMBHs is that the "occupation number," that is, the fraction of galaxies containing a seed-BH at high redshift, is highly model dependent. In other words, contributions to the EGB flux can potentially constrain seed-BH models. To this effect, our calculation for the initial density is a conservative value (see Sec. III D).

In Fig. 2 we show contributions to the EGB from DM annihilation into continuous gamma rays (we discuss monochromatic emission later). We use DM parameters $m_\chi = 100$ GeV and $\sigma\upsilon = 3 \times 10^{-26}$ cm^3 s^{-1}. The values of z_f and β in Table II were used. We do not expect low-redshift IMBHs to be resolved; it has been shown that GLAST will resolve minispikes in our galaxy and possibly Andromeda, but not further [21]. Moreover, we find that sources within $z = 0.01$ contribute less than a tenth of the total EGB contribution. We therefore show the flux, integrated safely from $z = 0$ to z_f. We find that minispikes

increase the gamma-ray flux from DM halos by 1–3 orders. In particular, scenario B can give fluxes that are of the order of current observations. Scenario A fluxes are two orders smaller, but we stress that scenario A is a conservative case, using the smallest IMBH mass and a mild $r^{-3/2}$ minispike. The "host halo only" is a prediction without any spikes nor minispikes, and therefore acts as a minimal prediction. The dashed curves indicate uncertainties caused by 1σ scatter in: $N_{bh,A}$ for scenario A, and $N_{bh,B}$ and z_{re} combined for scenario B.

In Fig. 3 we show how EGB contribution from scenario B depends on the free parameter β. As before, we use $z_{re} = 10.9$, $m_\chi = 100$ GeV, and $\sigma\upsilon = 3 \times 10^{-26}$ cm^3 s^{-1}. We show the 1σ scatter in $N_{bh,B}$ using vertical dashed lines. We find that our fitting is within 1σ error of EGRET observations.

B. Constraining DM parameters

Instead of performing a complete scan over DM parameters space, we follow Bertone et al. [21] and consider two discrete cases. In addition to our previously chosen set $m_\chi = 100$ GeV and $\sigma\upsilon = 3 \times 10^{-26}$ cm^3 s^{-1}, we define a new set $m_\chi = 1$ TeV and $\sigma\upsilon = 10^{-29}$ cm^3 s^{-1}. Using
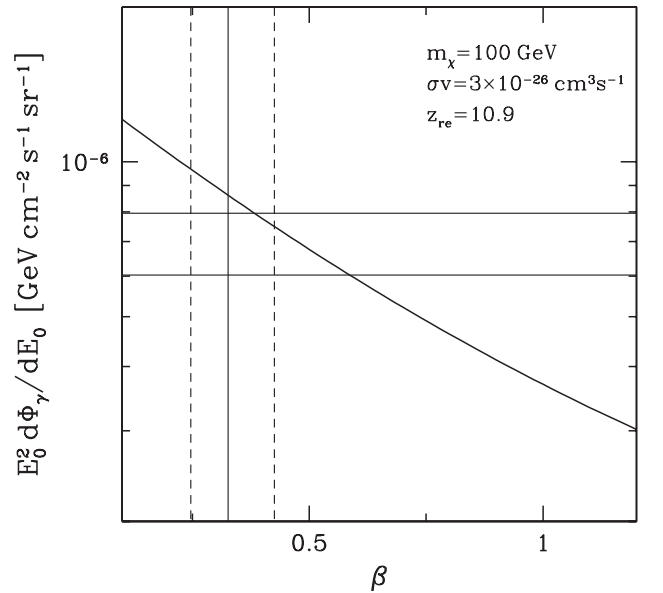
FIG. 3. Plot showing how EGB contributions from scenario B IMBH minispikes varies due β, the parameter of our IMBH number density fitting. Plotted is the flux at an energy of 1 GeV, where the contribution is greatest. The range of β determined from the 1σ scatter in $N_{\mathrm{bh},B}$ is shown by the vertical dashed lines. EGRET observations are shown by the horizontal rectangle.

scenario B with $z_{\mathrm{re}} = 10.9$ and $\beta = 0.3$, we plot in Fig. 4 the predicted EGB flux for both sets.

Now in Fig. 5 we show an advantage, from the point of view of constraining DM parameters, of considering
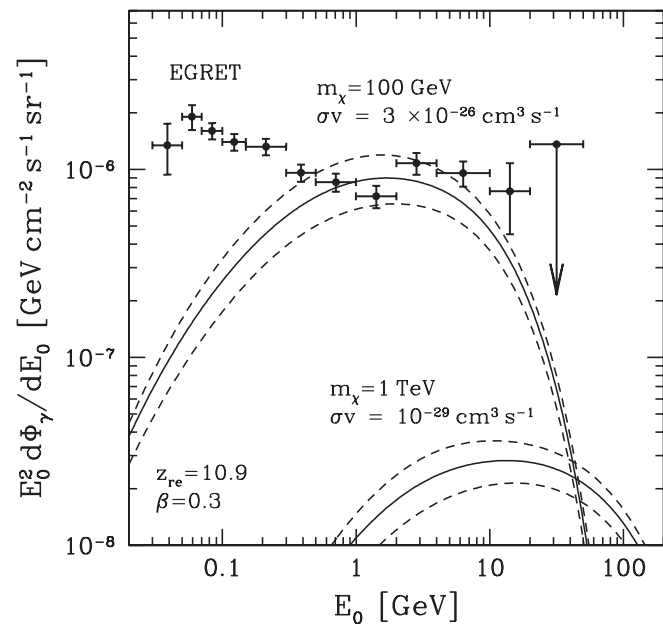

FIG. 4. Contributions to the EGB from scenario B IMBH minispikes, for two sets of DM parameters, the first with $m_\chi = 100$ GeV and $\sigma v = 3 \times 10^{-26}$ cm^3 s^{-1} and the second with $m_\chi = 1$ TeV and $\sigma v = 10^{-29}$ cm^3 s^{-1}. Errors include those from $N_{\mathrm{bh},B}$ and z_{re}.
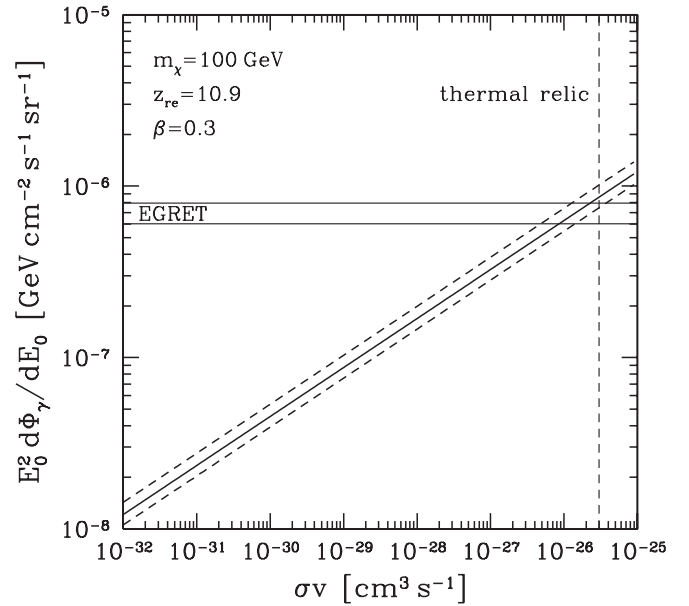

FIG. 5. Gamma-ray flux at $E = 1$ GeV from scenario B IMBHs, plotted against the annihilation cross section σv. The dashed lines indicate combined error in $N_{\mathrm{bh},B}$ and z_{re}. EGB observations by EGRET and σv of "natural" thermal neutralinos are shown. The weak dependency on σv works positively for DM detection.

IMBH minispike enhancements. We show contributions to the EGB at an energy of 1 GeV, against the DM annihilation cross section. As before, we use $z_{\mathrm{re}} = 10.9$ and $\beta = 0.3$, and assume for now $m_\chi = 100$ GeV. The advantage of minispikes is observed in the gradient of the plotted line. Although one would naively expect gamma-ray fluxes to scale as $\sigma v/m_\chi^2$, the presence of a minispike alters this dependence. This is due to the fact that the dominant term in the minispike enhancement [the integral in Eq. (15)] is given by the expression $\sim \rho_{\mathrm{lim}}^2 r_{\mathrm{lim}}^3$, which brings the gamma-ray flux scaling as $(\sigma v)^{2/7} m_\chi^{9/7}$, for minispikes growing out of a $\gamma = 1$ profile. Physically speaking, a smaller cross section works to maintain a denser minispike, which compensates for the decrease in flux due to the smaller cross section. One can say this weak dependence on DM parameters makes minispikes particularly suited for DM detection.

To determine the potential of the weak dependence on DM parameters, we consider gamma-ray observations by GLAST, which is expected to have more than an order better point source sensitivity than EGRET. With its launch, many gamma-ray sources that could not have been resolved until now will be detected, and taking these into account, a smaller EGB flux is expected. The most widely considered candidate for the dominant EGB contributor is unresolved blazars, i.e. a beamed population of active galactic nuclei (see [73] and references therein), and the fraction of these blazars that can be removed with GLAST depends on their luminosity function. The latest

calculation predicts that the resolvable fraction is around 20% [73]. If the EGB flux is entirely due to blazars, then the EGB will be reduced by the same fraction, and hence the sensitivity to σv will be improved by a factor of 2. We should, however, keep in mind that [73] concluded that blazars cannot fully explain the EGB flux, but only 25%–50%. Therefore, the remaining 50%–75% may be due to other astrophysical objects of either known or unknown origin, which may or may not be resolved by GLAST. This indicates that a significant fraction may still be resolved with GLAST, depending on the property of this additional contributor. In an optimistic case, where a fraction of $0.75 + 0.25 \times 0.2 = 0.8$ can be resolved with GLAST, the cross section sensitivity will be around 3×10^{-29} cm^{-2} s^{-1}, depending on values of z_f and N_{bh} (see error bars in Fig. 5). The sensitivity will also depend on M_{bh}; if halve M_{bh}, the sensitivity decreases to $\sim 10^{-28}$ cm^{-2} s^{-1}. These sensitivities are so small that no other experiments can compete in the next decades.

C. Line gamma rays

In the previous subsection we discussed constraining DM parameters using contributions to the EGB from DM annihilation into continuous photons, and highlighted its potential using the future GLAST mission. However, the continuum component lacks a distinguishing signature to separate it from other sources, such as unresolved blazars. Although the spectrum of other sources decreases rapidly at high energies, this is nonetheless a difficulty. Ideally, we would like to identify DM annihilation without these complications. The monochromatic component of DM annihilation provides a means of achieving this. As discussed earlier, the monochromatic emission provides a smoking-gun signature of DM annihilation due to its energy at the DM mass. Here, we present the monochromatic spectrum from the $\chi\bar{\chi} \rightarrow 2\gamma$ process with a fixed branching ratio of $b_{2\gamma} = 10^{-3}$. Our result is shown in Fig. 6 for two sets of DM parameters, $m_\chi = 100$ GeV and $\sigma v = 10^{-26}$ cm^3 s^{-1} (note this is not excluded by the continuum component), and $m_\chi = 1$ TeV and $\sigma v = 10^{-29}$ cm^3 s^{-1}. Again, we consider scenario B IMBH minispikes with $z_{re} = 10.9$ and $\beta = 0.3$.

The spectral shape of Fig. 6 arises because of distortion due to cosmological redshift and absorption of gamma rays during propagation. The larger peak at $E_0 = m_\chi$ is a characteristic of DM annihilation, and if detected provides very convincing evidence for DM. The smaller peak is a characteristic of IMBH minispikes; it is due to the strong enhancement factor at z_f, as shown in Fig. 1. If detected, this second peak identifies the presence of a high enhancement factor at high redshift, supporting the case of seed-BHs and minispikes.

In the past, line gamma rays had not been intensively considered, because the EGB spectrum taken by EGRET did not reach up to the required $O(100)$ GeV energies.
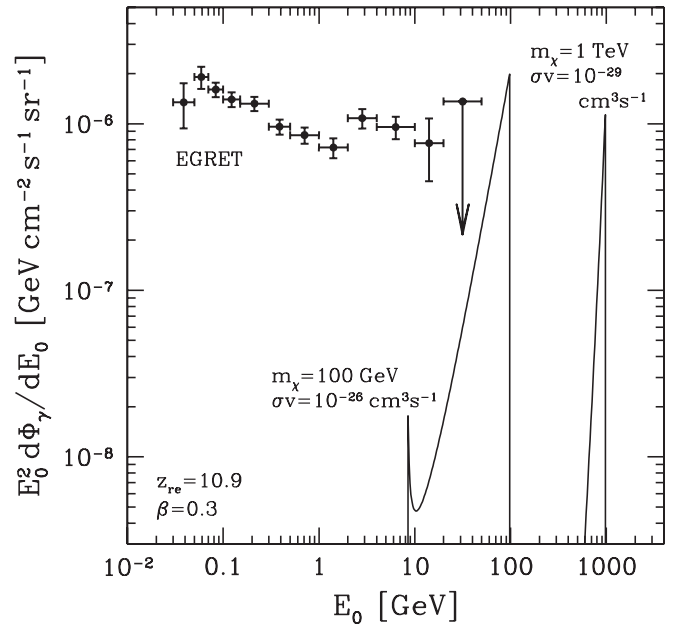

FIG. 6. Spectral signature in the EGB due to DM annihilation into monochromatic photons in scenario B IMBH minispikes. The 2γ branch is considered here, with a fixed branching ratio of 10^{-3}. Two DM parameters sets are shown, $m_\chi = 100$ GeV and $\sigma v = 10^{-26}$ cm^3 s^{-1} (this is not excluded by the continuum component), and $m_\chi = 1$ TeV and $\sigma v = 10^{-29}$ cm^3 s^{-1}. We used $z_{re} = 10.9$ and $\beta = 0.3$.

With GLAST however, the energy window extends up to 300 GeV (and with better energy resolution), and line gamma rays could be a serious candidate of the first DM detection. Furthermore, as shown in Fig. 6, the minispike around IMBHs provide such high EGB line fluxes that it might give better evidence than the continuum flux. The characteristic spectral feature, combined with good energy resolution of GLAST, work quite positively for the detection of line gamma rays, even if gamma rays from other astrophysical sources give considerable contribution at the same energy.

V. DISCUSSION AND CONCLUSIONS

We have studied contributions to the EGB from DM annihilation in minispikes around IMBHs. Our results are plotted in Fig. 2 using DM parameters $m_\chi = 100$ GeV and $\sigma v = 3 \times 10^{-26}$ cm^3 s^{-1}. We find that a consideration of minispikes increase the contribution by 1–3 orders, so that in optimistic scenarios the predicted gamma-ray flux may reach current EGB values. The EGB can therefore potentially be used to constrain DM parameters and/or IMBH scenarios, particularly when better EGB observations are taken by GLAST. In our work, we considered two IMBH formation scenarios, scenario A being remnants of Population-III stars [32], and scenario B being formed in the centers of protogalactic disks [33]. Scenario A is our conservative case (mass $10^2 M_\odot$ with a mild $r^{-3/2}$ minis-

pike) while scenario B is our optimistic (mass $10^5 M_\odot$ with a $r^{-7/3}$ minispike).

We also showed that DM annihilation into monochromatic gamma rays may be a serious contender for indirect DM detection. Our result, for scenario B IMBHs and two sets of DM parameters, is shown in Fig. 6. Note that these parameters were chosen so that it is not excluded by the continuum component. The higher energy peak, at an energy equivalent to the DM mass, is within GLAST's potential observation range, and can provide a potential smoking-gun signature in the EGB.

Compared to SMBH spikes, IMBH minispikes have the disadvantage that it is smaller, and it grows out of less dense DM profiles. Also, the survival probability of spikes and minispikes are still uncertain. However, there are still advantages to using IMBH minispikes. First, it has been shown that observations of our galaxy's center constrain the strength of spikes to such a degree that DM annihilation in spikes cannot significantly contribute to the EGB [29]. Second, although survival probabilities are uncertain, we can select IMBHs that are likely to have maintained their minispikes. Our selection involves choosing IMBHs that *have not experienced any mergers*, on the grounds that mergers strongly destroy DM enhancements. Additionally, such unmerged IMBHs are likely to reside in the outskirts of galactic halos, where it is not affected by dynamical processes that are also known to deplete DM enhancements.

It must also be added that minispike formation requires some initial conditions to be met, including an adiabatic and symmetric BH formation, formation of a BH in the center of its host halo, and very cold initial DM orbits near the halo center. These conditions are generally supported by the collisionless nature of particle DM, and adiabaticity is satisfied when one compares the BH formation time scale to the dynamical time scale at some relevant distance [21]. However, the collapse and accretion processes during BH formation are not well known, and are likely to be complex and far from symmetric. Also, we have neglected the effects of seed-BHs born with enough kick-recoil velocities to be expelled out of their host halos. Although a detailed study is beyond the scope of this paper, minispike formation for such seeds may be suppressed.

An advantage of DM detection using minispikes is the fact that the gamma-ray flux is weakly dependent on DM parameters. This is because the smaller the σv, the longer the minispike remains sharp. This fact compensates for the lack in flux, bringing the flux proportional to $(\sigma v)^{2/7} m_\chi^{9/7}$. As a consequence, GLAST may be able to probe down to $\sigma v \sim 10^{-29}$ cm^3 s^{-1} if we optimistically assume scenario B IMBH minispikes, and that 80% of the EGB is resolvable by GLAST. This is far smaller than any other experiment, and excludes the allowed σv region due to the standard thermal relic SUSY DM scenario. However, evidence concerning IMBH properties and EGB composition are required before setting such constraints. In this respect, it has recently been shown that the EGB power spectrum can be used to discriminate DM contributions from other sources [31].

All our calculations can be applied to other numerous DM candidates by simply substituting the appropriate differential gamma-ray spectrum per annihilation Eq. (4). A detailed search over particle DM candidates using EGB contributions should become possible with the launch of GLAST, and these should then be cross correlated with constraints from other potential DM signals. Finally, we have used EGB contributions to reveal DM properties, but we stress that the fact that scenario B predicts gamma-ray fluxes that are two orders greater than scenario A may also shed light on IMBH and SMBH models.

ACKNOWLEDGMENTS

[1] G. Jungman, M. Kamionkowski, and K. Griest, Phys. Rep. **267**, 195 (1996).

[2] L. Bergstrom, Rep. Prog. Phys. **63**, 793 (2000).

[3] G. Bertone, D. Hooper, and J. Silk, Phys. Rep. **405**, 279 (2005).

[4] http://glast.stanford.edu/.

[5] H. U. Bengtsson, P. Salati, and J. Silk, Nucl. Phys. **B346**, 129 (1990).

[6] V. Berezinsky, A. Bottino, and G. Mignola, Phys. Lett. B **325**, 136 (1994).

[7] L. Bergstrom and P. Ullio, Nucl. Phys. **B504**, 27 (1997).

[8] L. Bergstrom, P. Ullio, and J. H. Buckley, Astropart. Phys. **9**, 137 (1998).

[9] L. Bergstrom, J. Edsjo, and C. Gunnarsson, Phys. Rev. D **63**, 083515 (2001).

[10] A. Cesarini, F. Fucito, A. Lionetto, A. Morselli, and P. Ullio, Astropart. Phys. **21**, 267 (2004).

[11] D. Hooper, I. de la Calle Perez, J. Silk, F. Ferrer, and S. Sarkar, J. Cosmol. Astropart. Phys. 09 (2004) 002.

[12] N. Fornengo, L. Pieri, and S. Scopel, Phys. Rev. D **70**, 103529 (2004).

[13] D. Horns, Phys. Lett. B **607**, 225 (2005).

[14] P. Gondolo and J. Silk, Phys. Rev. Lett. **83**, 1719 (1999).

[15] P. Ullio, H. S. Zhao, and M. Kamionkowski, Phys. Rev. D **64**, 043504 (2001).

[16] D. Merritt, M. Milosavljevic, L. Verde, and R. Jimenez,

Phys. Rev. Lett. **88**, 191301 (2002).

[17] G. Bertone and D. Merritt, Phys. Rev. D **72**, 103502 (2005).

[18] D. Merritt, Phys. Rev. Lett. **92**, 201304 (2004).

[19] G. Zaharijas and D. Hooper, Phys. Rev. D **73**, 103501 (2006).

[20] M. C. Miller and E. J. M. Colbert, Int. J. Mod. Phys. D **13**, 1 (2004).

[21] G. Bertone, A. R. Zentner, and J. Silk, Phys. Rev. D **72**, 103517 (2005).

[22] P. Sreekumar *et al.* (EGRET Collaboration), Astrophys. J. **494**, 523 (1998).

[23] A. W. Strong, I. V. Moskalenko, and O. Reimer, Astrophys. J. **613**, 956 (2004).

[24] L. Bergstrom, J. Edsjo, and P. Ullio, Phys. Rev. Lett. **87**, 251301 (2001).

[25] P. Ullio, L. Bergstrom, J. Edsjo, and C. Lacey, Phys. Rev. D **66**, 123502 (2002).

[26] J. E. Taylor and J. Silk, Mon. Not. R. Astron. Soc. **339**, 505 (2003).

[27] D. Elsaesser and K. Mannheim, Astropart. Phys. **22**, 65 (2004).

[28] D. Elsaesser and K. Mannheim, Supersymmetric dark matter and the extragalactic gamma ray background (2005).

[29] S. Ando, Phys. Rev. Lett. **94**, 171303 (2005).

[30] T. Oda, T. Totani, and M. Nagashima, Astrophys. J. **633**, L65 (2005).

[31] S. Ando and E. Komatsu, Phys. Rev. D **73**, 023521 (2006).

[32] P. Madau and M. J. Rees, Astrophys. J. **551**, L27 (2001).

[33] S. M. Koushiappas, J. S. Bullock, and A. Dekel, Mon. Not. R. Astron. Soc. **354**, 292 (2004).

[34] K. Makishima *et al.*, Astrophys. J. **535**, 632 (2000).

[35] G. Fabbiano, Annu. Rev. Astron. Astrophys. **27**, 87 (1989).

[36] M. C. Begelman, Astrophys. J. **568**, L97 (2002).

[37] A. R. King, M. B. Davies, M. J. Ward, G. Fabbiano, and M. Elvis, Astrophys. J. **552**, L109 (2001).

[38] D. Elsaesser and K. Mannheim, Phys. Rev. Lett. **94**, 171302 (2005).

[39] J. M. Miller, A. C. Fabian, and M. C. Miller, Astrophys. J. **614**, L117 (2004).

[40] M. Cropper *et al.*, Mon. Not. R. Astron. Soc. **349**, 39 (2004).

[41] T. E. Strohmayer and R. F. Mushotzky, Astrophys. J. **586**, L61 (2003).

[42] X. Fan *et al.* (SDSS Collaboration), Astron. J. **122**, 2833 (2001).

[43] A. J. Barth, P. Martini, C. H. Nelson, and L. C. Ho, Astrophys. J. **594**, L95 (2003).

[44] C. J. Willott, R. J. McLure, and M. J. Jarvis, Astrophys. J. **587**, L15 (2003).

[45] Z. Haiman and A. Loeb, Astrophys. J. **552**, 459 (2001).

[46] X.-H. Fan *et al.* (SDSS Collaboration), Astron. J. **131**, 1203 (2006).

[47] R. R. Islam, J. E. Taylor, and J. Silk, Mon. Not. R. Astron. Soc. **340**, 647 (2003).

[48] S. M. Koushiappas and A. R. Zentner, Astrophys. J. **639**, 7 (2006).

[49] M. Volonteri, F. Haardt, and P. Madau, Astrophys. J. **582**, 559 (2003).

[50] T. Matsubayashi, H. Shinkai, and T. Ebisuzaki, Astrophys. J. **614**, 864 (2004).

[51] C. L. Fryer, S. E. Woosley, and A. Heger, Astrophys. J. **550**, 372 (2001).

[52] J. R. Bond, W. D. Arnett, and B. J. Carr, Astrophys. J. **280**, 825 (1984).

[53] F. Nakamura and M. Umemura, Astrophys. J. **548**, 19 (2001).

[54] H. S. Zhao and J. Silk, Phys. Rev. Lett. **95**, 011301 (2005).

[55] M. Tegmark *et al.*, Astrophys. J. **474**, 1 (1997).

[56] A. R. Zentner, A. A. Berlind, J. S. Bullock, A. V. Kravtsov, and R. H. Wechsler, Astrophys. J. **624**, 505 (2005).

[57] M. H. Salamon and F. W. Stecker, Astrophys. J. **493**, 547 (1998).

[58] J. F. Navarro, C. S. Frenk, and S. D. M. White, Astrophys. J. **462**, 563 (1996).

[59] B. Moore, T. Quinn, F. Governato, J. Stadel, and G. Lake, Mon. Not. R. Astron. Soc. **310**, 1147 (1999).

[60] D. Merritt, A. W. Graham, B. Moore, J. Diemand, and B. Terzic, astro-ph/0509417.

[61] J. Diemand, B. Moore, and J. Stadel, Mon. Not. R. Astron. Soc. **353**, 624 (2004).

[62] J. F. Navarro *et al.*, Mon. Not. R. Astron. Soc. **349**, 1039 (2004).

[63] T. Fukushige, A. Kawai, and J. Makino, Astrophys. J. **606**, 625 (2004).

[64] D. Merritt, astro-ph/0301257.

[65] T. Abel, G. L. Bryan, and M. L. Norman, Science **295**, 93 (2002).

[66] V. Bromm, P. S. Coppi, and R. B. Larson, Astrophys. J. **564**, 23 (2002).

[67] P. J. E. Peebles, Gen. Relativ. Gravit. **3**, 63 (1972).

[68] G. D. Quinlan, L. Hernquist, and S. Sigurdsson, Astrophys. J. **440**, 554 (1995).

[69] W. H. Press and P. Schechter, Astrophys. J. **187**, 425 (1974).

[70] R. K. Sheth, H. J. Mo, and G. Tormen, Mon. Not. R. Astron. Soc. **323**, 1 (2001).

[71] A. Jenkins *et al.* (Virgo Consortium), Astrophys. J. **499**, 20 (1998).

[72] L. Page *et al.*, astro-ph/0603450.

[73] T. Narumoto and T. Totani, Astrophys. J. **643**, 81 (2006).